Molecular Mobility of Amorphous Chain Segments of Ethylene−Methyl Methacrylate Copolymer Films as a Function of Temperature Estimated by Positron Annihilation, X-ray Diffraction, and ^{13}C NMR

Lin Ma,[†] Chunqing He,[‡] Takenori Suzuki,[‡] Mami Azuma,[†] Yuezhen Bin,[†] Hiromichi Kurosu,[†] and Masaru Matsuo*[,†]

Textile and Apparel Science, Faculty of Human Life and Environment, Nara Women's University, Nara 630-8263 Japan, and Radiation Science Center of High Energy Accelerator Research, Organization 1-1 Oho, Tsukuba, Ibaraki 305-0801, Japan

Received September 30, 2002

ABSTRACT: The relationship between the morphology and the mechanical properties of copolymer ethylene−methyl methacrylate (EMMA) films with different MMA contents was investigated as a function of temperature by using positron annihilation, X-ray diffraction, and ^{13}C solid-state NMR. To make clear the effect of MMA side groups on the morphology and molecular mobility of EMMA as a function of temperature, the characteristics of EMMA were discussed together with those of copolymer (dimethylamino)ethyl methacrylate (EDAM) and branched polyethylene. Three kinds of transitions were confirmed by positron annihilation: the first at temperatures around −130 °C, the second around −40 °C, and the third around 50 °C. The first and the second transitions were due to the commencement of molecular motions, which can remove trapped electrons from their shallow potentials, while the third transition around 50 °C was attributed to the partial melting of unstable small crystallites. These transitions were in good agreement with the results obtained from differential scanning calorimetry (DSC) and X-ray measurements. Namely, the DSC curves of EMMA provided a peak around −25 to − 30 °C corresponding to the second transition and a small peak around 43−48 °C corresponding to the third transition. Lifetime (τ_3) showed no obvious change between branched polyethylene and EMMA-I melt films. This result can be explained within the framework of the spur model of Ps formation in terms of the trapping of positrons (and may be electrons) by the polar groups, −C═O, in EMMA.

I. Introduction

In the previous paper,[1] the effect of side groups on the crystallization of ethylene main chains was investigated by using ethylene−methyl methacrylate (EMMA), which is a copolymer of ethylene and methyl methacrylate (MMA) manufactured by a high-pressure radical polymerization process common to low-density polyethylene (LDPE). The relationship between the morphology and the mechanical properties of copolymer ethylene−methyl methacrylate (EMMA) was estimated as a function of temperature by using polarized light scattering, X-ray diffraction, and ^{13}C solid-state NMR. Parameters of the Laue function and the structural factor determined on the basis of X-ray indicated that EMMA films, crystallinity being less than 10% and MMA content being about 14 mol %, have unstable crystallites with crystal size of about 3 nm and large fluctuations in crystal lattice distances. On the other hand, the longer ethylene sequences in the noncrystalline phase had a nonrandom local arrangement. It is evident that the bulky volume of the MMA side groups suppresses crystallization of ethylene sequences. Consequently, even though crystallization is suppressed, the tendency for longer ethylene sequences to self-order leads to a dynamic local ordering in the noncrystalline phase.

Recent investigation of positron annihilation has given excellent information for characterization of several kinds of polymers. For example, Liu et al.[2] studied the free volume distribution of polystyrene. They pointed out that the distributions of free volume fractions fit well with the theoretical function according to the Shimha−Somcynsky lattice model[3] through the comparison with the experimental results obtained using photochromic and fluorescent probes as well as with the Turnbell−Cohen free volume theory.[4,5] Furthermore, Suvegh et al.[6] studied free volume distribution in monodisperse and polydisperse poly(methyl methacrylate). Their results for lifetime measurement revealed that the free volume holes are smaller and their distribution is narrower in monodisperse samples compared with polydisperse samples.

There is another aspect in positron annihilation. Positrons injected into polymer samples can be used as a probe to study the characteristics as shown above and also give radiation effect to the samples itself. From the effect, electrons and positive ions are created. These excited electrons have been studied by Keyser et al.[7] by using γ-irradiated polyethylene: at 77 K, most of polymer motions (rotational motion and micro-Brownian motion) are frozen, and then potentials which can trap electrons are formed. The binding energy of these trapped electrons is so small (i.e., shallow potential) that they are easily excited by low-energy photons (light bleaching) even with energy of less than 1 eV. Also, they can be easily picked up by injected positrons, resulting in the increase in the formation of positronium (Ps), which is a hydrogen-like atom being composed of an electron and positron.

Despite the many studies on (dimethylamino)ethyl methacrylate (EDAM),[8−10] few papers have examined

* To whom all correspondence should be addressed: Fax 81-742-20-3462; e-mail m-matsuo@cc.nara-un.ac.jp.
[†] Nara Women's University.
[‡] Radiation Science Center of High Energy Accelerator Research.

10.1021/ma021543r CCC: $25.00
Published on Web 09/17/2003

Table 1. Characterization of EMMA and EDAM

specimen	mol %	melting point (°C)	draw ratio (max)	molecular weight $M_n(10^4)$	$M_w(10^4)$
EMMA-I(WD201)	3.0	100	5	4.7	
EMMA-II(WH202)	6.5	85	6	4.3	
EMMA-III(WM403)	14.6	64	10	3.1	
EDAM-I(DA3023)	3.9	97	1.6	2.43	8.88
EDAM-II(DA3031)	4.1	66	1.6	2.93	8.29
LDPE (G201)	5.3[a]	104	4.6	4.13[b]	

[a] 2.8 CH_3/100 C. [b] M_v (10^4).

the detailed morphology and mechanical properties of EMMA films with different MMA contents.[1,11] As part of a series of papers dealing with EMMA, these studies are done to elucidate the important relationship between morphology and molecular dynamics of ethylene sequences interrupted by large MMA side groups. The results are compared with the characteristics of EDAM and branched polyethylene. Our characteristics were done as a function of temperature using positron annihilation, X-ray, and ^{13}C NMR measurements.

II. Experimental Section

Experimental Procedure. Characteristics of Sample. EMMA, EDAM random copolymer, and branched PE (G201) samples were furnished by Sumitomo Chemical Co. Ltd. The chemical structures and the characteristics of the samples are listed in Table 1. The designation in parentheses such as WD201 and DA3023 are commercial names.

X-ray. The X-ray measurements were carried out with a 12 kW rotating-anode X-ray generator (Rigaku RAD-rA). The X-ray beam by Cu Kα radiation at 200 mA and 40 kV was monochromatized with a curved graphite monochromator. The WAXD intensity distribution was obtained at desired temperatures from −110 to 60 °C using a curved position-sensitive proportional counter (PSPC). To pursue the accuracy of accumulation of the intensity, the measured period was set to be 10 min.

^{13}C NMR. NMR measurements as a function of temperature were carried out for the EMMA melt films on a JEOL JM-EX 270 spectrometer, operating at 67.8 MHz for ^{13}C. Room temperature and 55 °C measurements were performed. The actual temperatures in the probe under spinning were confirmed to be in the ranges 27−36 and 55−60 °C, respectively. The magic-angle spinning rate was 5−5.5 kHz. As for ^{13}C CP (cross-polarization)/MAS measurements, the pulse width of ^1H, the repeated time, and the contact time were set to be 4.9−5.1 μs, 5 s, and 2 ms, respectively. The accumulation number was 1000−3000. For ^{13}C PST (pulse saturation transfer)/MAS, the pulse widths of ^1H and ^{13}C were 4.6−5.1 and 4−5.6 μs, respectively. The repeated irradiation cycle of ^1H pulse width and the repeated irradiation number of ^1H pulse were 10 ms and 500 times, respectively. The accumulation number was 2400. The chemical shifts were determined relative to the higher field signal (29.5 ppm) of adamantane.

Positron Annihilation. Positron annihilation experiments were conducted with a conventional fast−fast coincidence system having a time resolution of 300 ps full width at half-maximum (fwhm). The time spectrometer was composed of two plastic scintillation detectors (40 mm diameter × 40 mm Pilot-U mounted on a Hamamatsu H1949 photomultiplier), two differential constant fraction discriminators (ORTEC 583) (one for start signals from 1.27 MeV γ-rays and the other one for stop signals from 0.511 MeV annihilation γ-rays), a time-to-amplitude converter (ORTEC 4570), and a multichannel analyzer with a 1024 conversion gain (SEIKO 7800). The data taking was controlled by a personal computer (NEC-PC).

A position source was prepared by depositing ca. 1.1 MBq (30 μCi) of aqueous $^{22}NaCl$ on a Kapton foil of 7 μm thickness and 10 × 10 mm area. After drying, the foil was covered with the same size of foil, and the edges were glued with epoxy resin. The source was further sealed in a 3 μm Mylar foil and then sandwiched by two identical samples for positron-annihilation measurements. The diameter of the spot of the ^{22}Na source was ca. 2 mm. During the measurement, samples were kept in a vacuum cell, in which their temperature was controlled. Spectra were recorded every hour, and about 1−2 million events were stored in each spectrum. Thus, a positron-annihilation spectrum with sufficient statistics to decompose the orthopositron (o-Ps) component was obtained.

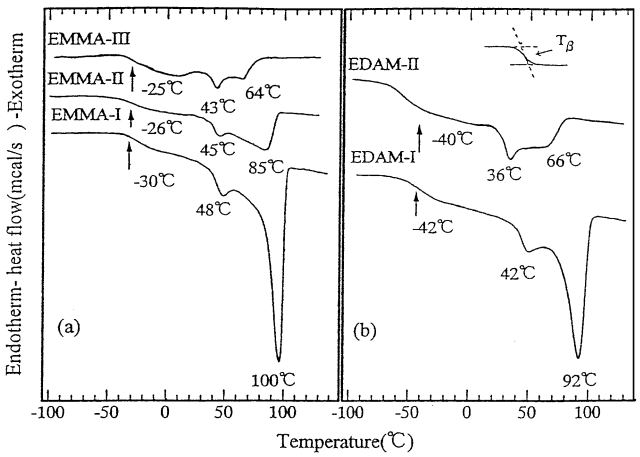

Figure 1. DSC curves: (a) EMMA films and (b) EDAM films.

Viscoelastic Measurements. The complex dynamic tensile modulus was measured at 10 Hz over the temperature range from −150 to 300 °C by using a viscoelastic spectrometer (VES-F) obtained from Iwamoto Machine Co. Ltd. The length of the specimen between the jaws was 40 mm, and the width was about 1.5 mm. During measurements, the specimen was subjected to a static tensile strain in the range 0.05−0.1% to place the sample in tension during the axial sinusoidal oscillation. The complex dynamic modulus was measured by imposing a small dynamic strain to ensure linear viscoelastic behavior of the specimen.[12]

DSC Measurements. The calorimetric investigations of EMMA and EDAM specimens were performed with an Exstar 6000 of Seiko Instrument Inc. The heating rate was 1 °C min^{-1}. The weight of specimen was 10 mg.

III. Results and Discussion

Figure 1 shows DSC curves for EMMA and EDAM films. In all cases, the profile shows a single main peak in addition to a small peak at lower temperature side. As can be seen in this figure, the position of the main peak shifts to lower temperature side with increasing the content of the side groups, indicating the existence of smaller size crystallites and lower crystallinity. This tendency is in good agreement with the results obtained by X-ray and ^{13}C NMR. Actually, the peak of branched polyethylene (G201) appeared at 104 °C,[13] much higher than the corresponding peak temperature shown in this figure. The small peak of EMMA around 43−48 °C and that of EDAM around 36−42 °C are thought to be due to the partial melting of the very small unstable crystallites. Every peak appeared above room temperature shifts to lower temperature side as the content of side groups increases. This indicates that at elevated temperature the activity of molecular motions in the crystallites become more pronounced with increasing side group content, since the crystal size becomes smaller and the fluctuation of the lattice distance becomes larger. This phenomenon will be analyzed in detail using positron annihilation, X-ray, and ^{13}C NMR, thereby relating the fluctuations in crystal size with molecular mobility.

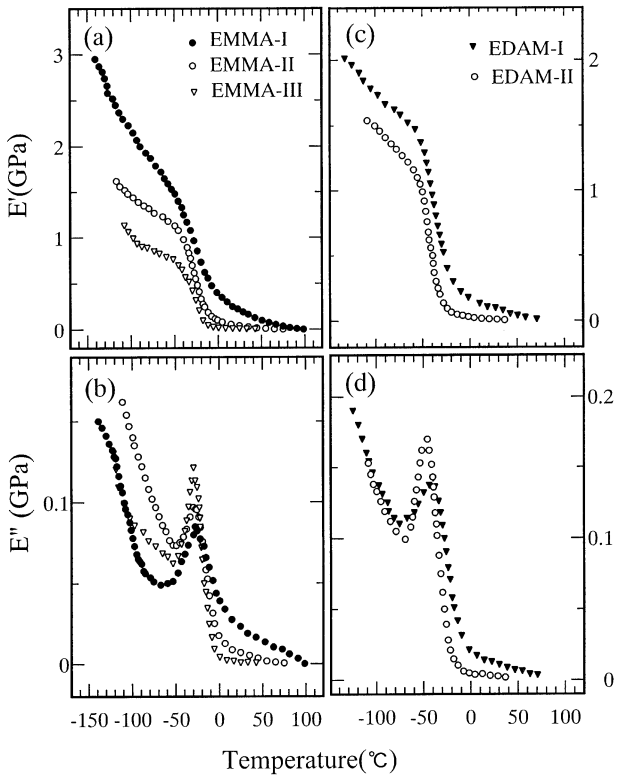

Figure 2. Temperature dependence of the storage and loss moduli for EMMA and EDAM films.

Figure 2 shows the temperature dependence of the storage modulus (E') and the loss modulus (E'') at a frequency of 10 Hz measured for three kinds of EMMA (EMMA-I, EMMA-II, and EMMA-III) and two kinds of EDAM (EDAM-I and EDAM-II). For normal linear polyethylene (PE) specimens, it is well-known that there exist the α, β, and γ relaxations. However, for the EMMA and EDAM films, the α dispersion associated with crystal relaxation cannot be observed because of low crystallinity, while a clear dispersion peak of the β relaxation could be observed. Following Kawai et al.,[14,15] the β dispersion of polyethylene is assigned as interlamellar grain boundary phenomena associated with orientational and distortional dispersions of noncrystalline phases between lamellae within spherulites. The conclusion was derived from the information concerning the combination of the experimental results measured by dynamic X-ray and dynamic birefringence techniques. On the other hand, Matsuo et al.[16] pointed out that the β dispersion is due to a large movement of amorphous chains based on the experimental results measured by dynamic mechanical and positron annihilation techniques. The γ dispersion, associated with the motion of a short chain segment in the amorphous phase,[17] is not observed. Judging from the γ dispersion peak of polyethylene, it is evident that the γ dispersion peak probably appears at temperature < -150 °C. Unfortunately, E' and E'' measurements at temperature < -150 °C cannot be done by using the present viscoelastic spectrometer (VES-F).

On the basis of the results, the frequency dependence of E' and E'' for EMMA-III and EDAM-II was measured in the temperature range from −80 to 10 °C to pursue a detailed analysis of the β relaxation, and the master curves of E' and E'' against frequency were obtained by shifting horizontally until good superposition is achieved. The logarithm of the temperature dependence

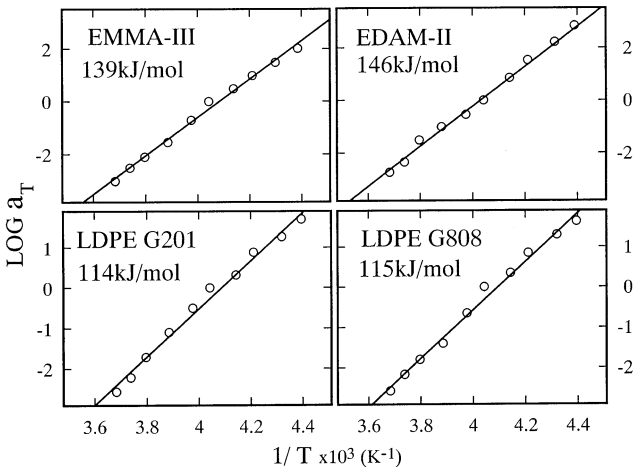

Figure 3. Activation energies for the EMMA-III, EDAM-II, and LDPE films.

of the horizontal shift factor $a_T(T,T_0)$ was plotted against reciprocal absolute temperature, as shown in Figure 3. The same measurement was done for the branched polyethylene films (G201 and G808). The Arrhenius plots thus obtained are represented by a straight line. The activation energies obtained from the slopes of these lines are represented in each column. These activation energies are higher than the values (114−115 kJ/mol) for branched polyethylene films (G201 and G808) measured by preliminary experiments. The value for the film (G201) is slightly higher than values obtained by Kawai et al.[14] Anyway, it is obvious that the mobility of the amorphous chain segments becomes less pronounced with increasing comonomer contents. Judging from the activation energy of the β relaxation close to that (about 120 kJ/mol) of the α_1 relaxation, the β mechanical relaxation for EMMA, EDAM, and PE can be assigned to the large movement of amorphous chains rather than the glass transition. Following Kawai et al.,[14] the energy of the β relaxation for linear polyethylene films became lower as crystallinity increased. Namely, the distinction between the α_1 and β mechanical relaxations of G201 with low crystallinity was reported to be impossible from the difference between their activation energies, since the both energies were almost the same.

According to the previous paper,[1] the X-ray and ^{13}C NMR measurements indicated that the MMA side groups with bulky volume suppress the crystallization that is otherwise an essential property of ethylene sequences. Then the difficulty in assembling available ethylene sequences into true crystallites leads to a local ordered arrangement of the ethylene sequences rather than a random orientation in the noncrystalline phase. If this is the case, the high activation energies obtained for the β relaxation are reasonable. This is due to the fact that mobility of those EMMA and EDAM chain segments having a local ordered arrangement are less pronounced than that of PE chain segments with a random orientation.

Chain motion in the amorphous phase and the glass transition in high-density polyethylene (HDPE) were studied by Hentschel et al.,[18] using variable-temperature ^2H NMR. The spectral change from −163 to 37 °C was analyzed in terms of free volume picture relating to thermal expansion in the amorphous region. They pointed out that the increase in the number of free volume holes provides an increase in the number of

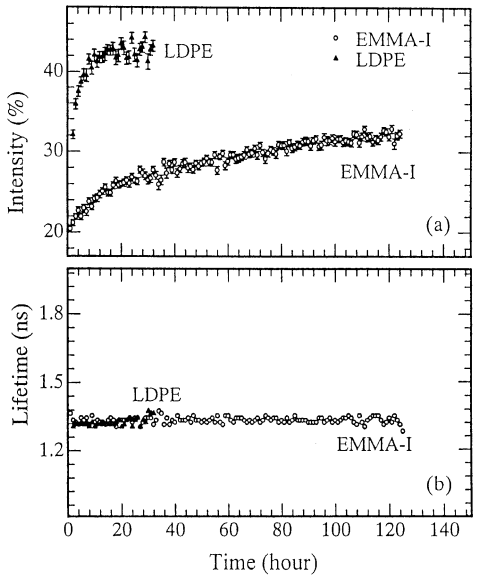

Figure 4. Intensity (I_3) and lifetime (τ_3) of long-lived component of the orthopositronium (o-Ps) as a function of time for EMMA-I and LDPE films.

conformations accessible to molecular motion. They suggested three bond motions at low temperatures, five-bond motions at room temperature, and motions with more than 10 bonds below the melting point.

An increase in the average free volume holes can be clearly monitored by positron annihilation.[19] Positron annihilation is one of the useful techniques to investigate relaxation characteristics of polymers.[20−26] Positrons emitted from ^{22}Na induce radiation effect on polymer samples, and then resultant electrons are excited from the constituent atoms. These electrons are trapped in a shallow potential, which are formed at low temperature far below the glass temperature (T_g). The increase in the number of these trapped electrons is observed as an increase in the intensity (I_3) of the long-lived component of orthopositronium (o-Ps).

According to published results of PAL measurements, the intensity (I_3) of the long-lived component is dependent on the crystallinity,[27] the degree of cross-links, the conditions of polymerization,[28] and the radiation effects, induced by positron irradiation.[29] Parts a and b of Figure 4 show intensity (I_3) and lifetime (τ_3) of long-lived components (o-Ps) for LDPE and EMMA-I melt films at −240 °C. Copolymer EMMA-I (3 mol % MMA content) was used to study the oxygen effect on positron annihilation. The increase in intensity (I_3) has been explained by an accumulation of trapped electrons in shallow traps, which are created after freezing the molecular motions at low temperature. For the branched PE (G201), intensity (I_3) attained saturation at 40% after 10 h of measurements, while the intensity (I_3) of EMMA-I attains 30% after 120 h of measurements. The lifetime (τ_3) shows no obvious change between these two samples. This result can be explained within the framework of the spur model[30,31] of o-Ps formation in terms of the trapping of positrons (and may be electrons) by the polar groups, −C═O, in EMMA.[32−34] Here we shall briefly discuss the basis. The intensity of o-Ps in polymers is well-known to be affected by the amount of free volume, crystallinity, cross-linking, radiation effects (radicals, trapped electrons), negative polar groups, diffusion length of positron, etc. If there is no trapped electron and positron trapping, according to the spur model, the probability of o-Ps formation depends on the structure of the polymer within a positron terminal spur. The latter is formed at the end of a positron trajectory and consists of positron, electrons, and ions. Figure 4 shows the elapsed time dependence of I_3; the positronium intensity I_3 is determined by the number of trapped electrons that can be picked up by a positron to form positronium. Positronium formation is inhibited by the polar group $-^{+}C{=}O^{-}$, since positrons can be trapped by $-^{+}C{=}O^{-}$ which has been reported.[32−34] Mobility of a positron also plays an important role on positronium formation, but its mobility is also affected by the availability of polar groups due to positron trapping. Therefore, −C═O plays a major role in the increase of I_3.

Copolymer EMMA-I (3 mol % MMA content) was used to study the oxygen effect on positron annihilation. Comonomer MMA consists of C, H, and O atoms. Particularly, it includes polar −C═O groups. Positrons injected in PMMA produce a terminal spur, which forms at the end of the slowing down process after most of the initial energy is lost. Nearly thermalized positrons in the terminal spur can pick up spur electrons and form positroniums. Incidentally, the spur electrons are produced by the ionizing action of incident positrons inside terminal spurs. During this migration, some of the positrons can be trapped by −C═O groups and annihilate with an electron on an O atom, which demonstrates the effect of oxygen at room temperature. This result indicates that a large number of free positrons annihilate on oxygen in EMMA. This suggests that a small fraction of polar, oxygen-containing groups in a copolymer structure gives a large oxygen effect even at room temperature. The obtained result may also imply that the amount of o-Ps in EMMA would be essentially higher if the trapping of positrons by oxygen were absent: the e^{+}−C═O bound state is considered to be stable even at room temperature.

In the case of PE, a fast increase in I_3 at −240 °C in comparison with the value for EMMA has been explained in terms of the storage of weakly bound electrons and the high mobility of positrons in PE. Positrons can move out of a terminal spur whose size is about 5−10 nm and diffuse to a distance up to about 70 nm[35] during which positrons can meet trapped electrons. This phenomenon causes an increase of o-Ps formation. However, in the case of EMMA, the positron diffusion length is expected to be shorter due to the trapping of positrons by polar −C═O; thus, positrons do not have sufficient time to meet weakly bound electrons. The results of Hirade et al.[36] show that the same increase (∼12%) of o-Ps formation in EMMA requires nearly 100 times higher concentrations of weakly bound electrons ($\sim 10^{17}$ cm^{-3}) than in the case of PE. Hence, o-Ps formation is limited to within a limited space, and the slowly increasing rate of o-Ps formation is related to the necessity of accumulating a higher densities of trapped electrons within a smaller space.[37]

Figure 5 shows temperature-dependent intensity (I_3) and lifetime (τ_3) of long-lived components (o-Ps) for EMMA-I melt films, where data are taken in dark (a) or with light on (b). The light came from an electric lamp outside of the cryostat through a glass window. Lifetime (τ_3) was almost the same for these two different measurement conditions, but the intensity (I_3) was quite different. The experiments were done to understand the different saturation behavior of trapped electrons.

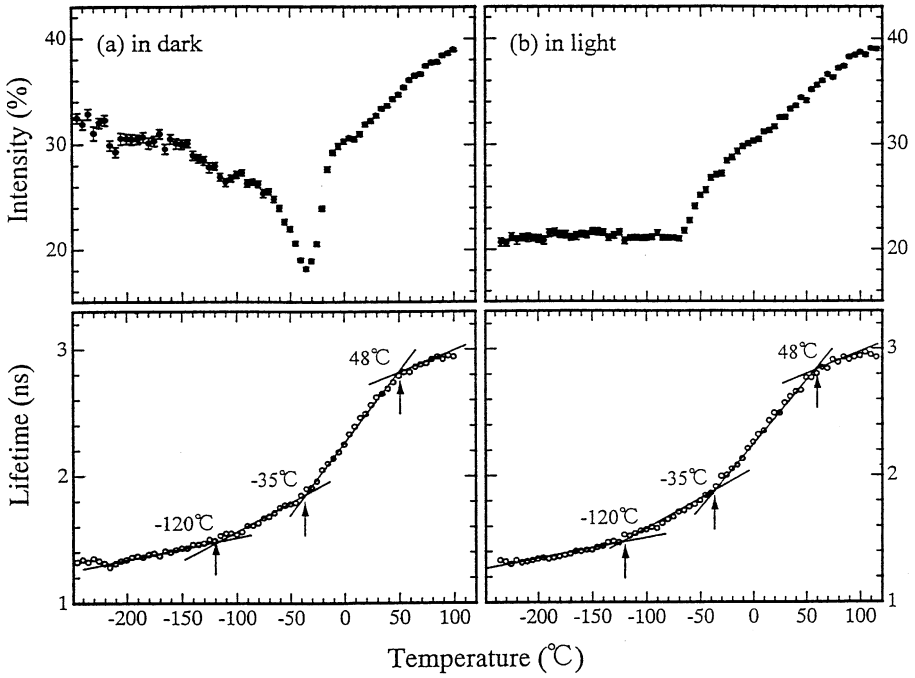

Figure 5. Intensity (I_3) and lifetime (τ_3) of the long-lived component of the orthopositronium (o-Ps) as a function of temperature for EMMA-I film.

In Figure 5a, the intensity was about 32% at −240 °C. This increase has been explained by an accumulation of trapped electrons in shallow traps[35,38] (about 1 eV), which are created after freezing the molecular motions at low temperatures (−170 °C or below). The positron irradiation was done for a week to reach saturation of trapped electrons at −240 °C. The secondary electrons that escape from the positron spur can be easily trapped in shallow potentials formed between polymer chains when the motions of the molecular chains and groups are frozen at low temperature. Accordingly, intensity (I_3) maintains a constant value up to −130 °C.

After being exposed to white light, as shown in Figure 5b, the intensity (I_3) decreased remarkably and reached a constant value of 20% after 10 h. This has been explained by bleaching of the trapped electrons. The large decrease in intensity (I_3) is due to the light bleaching of trapped electrons.[29,36] Accordingly, the increase in o-Ps formation in the dark is explained by an accumulation of trapped electrons.

In Figure 5a, it is seen that beyond −130 °C I_3 begins to decrease with increasing temperature and attains a minimum at about −35 °C. This is due to the fact that activation of molecular chain and group motion can bleach the trapped electrons with increasing temperature,[39] and consequently the o-Ps intensity would be greatly reduced. After the saturation, the temperature increased. The variation of I_3 shows a "V"-shape with a minimum value at −35 °C.

Positron annihilation can detect the motion of polymer chains and groups at low temperature by the variation of the o-Ps intensity. In accordance with Suzuki et al.,[40] the minimum temperature of I_3 is due to the fact that the local motion causes a large (macro-Brownian) movement of polymer chains in the amorphous phase. Accordingly, most of shallow potentials may be smeared out by the movement; the trapped electrons may then also disappear. If this is the case, the molecular motion at low-temperature affects the

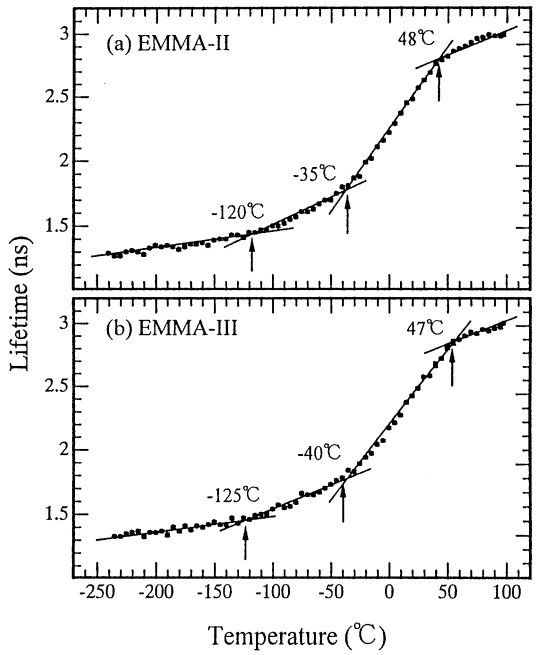

Figure 6. Lifetime (τ_3) of the long-lived component of the orthopositronium (o-Ps) as a function of temperature for EMMA-II and EMMA-III films.

trapped electrons in a shallow potential; consequently, the variation in I_3 is closely related to the relaxation temperature as a secondary effect. Beyond −35 °C, I_3 increases again. As discussed before, this is due to an apparent increase in the number of holes detected by positron annihilation because of the thermal expansion of the holes at elevated temperatures. In other word, the very small holes, which could not previously be detected by positron annihilation, can now be detected by an increase in the hole size upon thermal expansion.

Figure 6 shows τ_3 (lifetime of positronium) in the dark as a function of temperature estimated for two kinds of EMMA films, EMMA-II and EMMA-III. Figure 7 shows

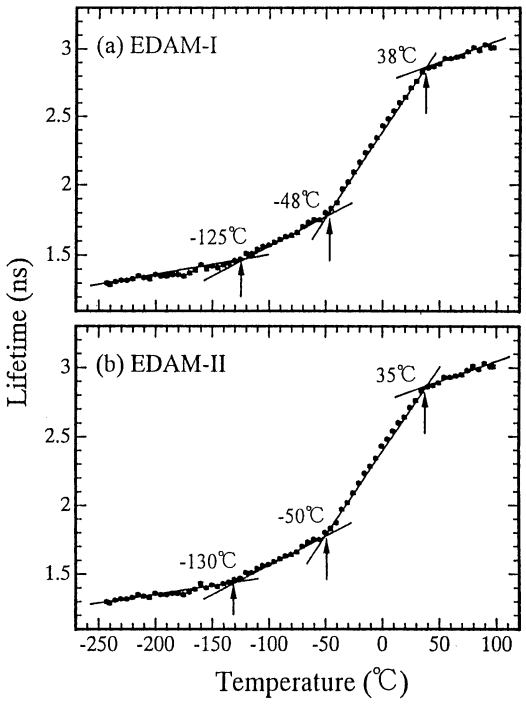

Figure 7. Lifetime (τ_3) of the long-lived component of the orthopositronium (o-Ps) as a function of temperature for EDAM-I and EDAM-II films.

τ_3 (lifetime of positronium) as a function of temperature estimated for two kinds of EDAM films, EDAM-I and EDAM-II. The lifetime τ_3 is well-known to be related to the size of hole by using Tao's equation.[17] The longer is τ_3, the bigger is the hole size in polymer solid. As shown in Figures 5−7, there exist three transitions of τ_3. The first transition at about −125 °C corresponds to the glass transition (the γ relaxation) associated with an increase in free volume, and the second transition at about −40 °C corresponds to the β relaxation. The two transitions of τ_3 show good correlation with the behavior of I_3. The third transition around 50 °C for EMMA and that around 40 °C for EDAM are attributed to the partial melting of very small unstable crystallites. In preliminary experiments, the third transition was observed for branched polyethylene (G201) with 38% crystallinity but not for linear polyethylene with crystallinity > 70%.

Figures 8 and 9 show the histograms of the lifetime distribution calculated by using maximum entropy for lifetime analysis (MELT)[41] for lifetime spectra obtained for the EMMA and EDAM films, respectively. The horizontal scale is also given as the radius of free volume calculated by Tao's equation.[19] The sharp intensity distribution indicates a narrow distribution of holes with relatively uniform size. As can be seen in figures, the distribution becomes broader and the peak top shifts to higher values of τ_3 with increasing temperature. This indicates that free volume holes within the specimen become bigger and have a wider size distribution with increasing temperature.

Returning to Figure 1, the DSC curves do not include temperatures around −150 °C associated with the γ dispersion; however, data show a transition around −42 to −25 °C associated with the β dispersion for EMMA and EDAM films. The transition for EMMA-I film appears clearly as the valley denoting the minimum point of I_3 shown in Figure 5a. As discussed before, a

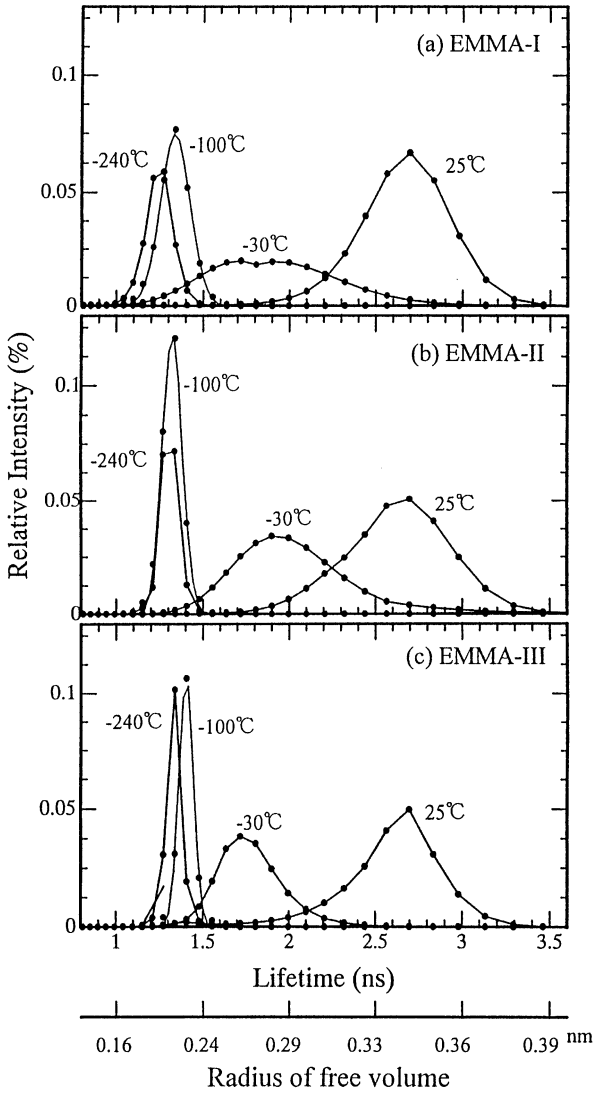

Figure 8. Histograms of the lifetime distribution for EMMA films at the indicated temperatures.

small peak in each DSC curve can be observed around 36−48 °C. This peak corresponds to the third transition of τ_3. Accordingly, it may be expected that this small peak in the DSC curve is due to partial melting of crystallites within the EMMA and EDAM specimens. Despite the appearance of the third transition of for τ_3, for branched PE (G201), EMMA, and EDAM, an indistinct shoulder or a peak at temperatures < 50 °C has never been observed in a DSC curve of branched PE (G201) films. The clear appearance of EMMA and EDAM films is obviously due to the active molecular mobility of molecular chains appeared by partial melting of unstable small crystallites in the temperature range 36−48 °C. This is due to the fact that the crystallites within EMMA and EDAM films are in a more unstable state than those within branched PE (G201).

Table 2 summarizes the transitions estimated by positron annihilation, the viscoelastic spectrometer, and DSC curves. The second transition temperature of the positron annihilation data is in good agreement with the β peak temperature observed by viscoelastic measurements. The first transition temperature is probably thought to be due to the γ dispersion, but the γ dispersion peak could not be observed by the viscoelastic spectrometer. The third transition is in good agreement

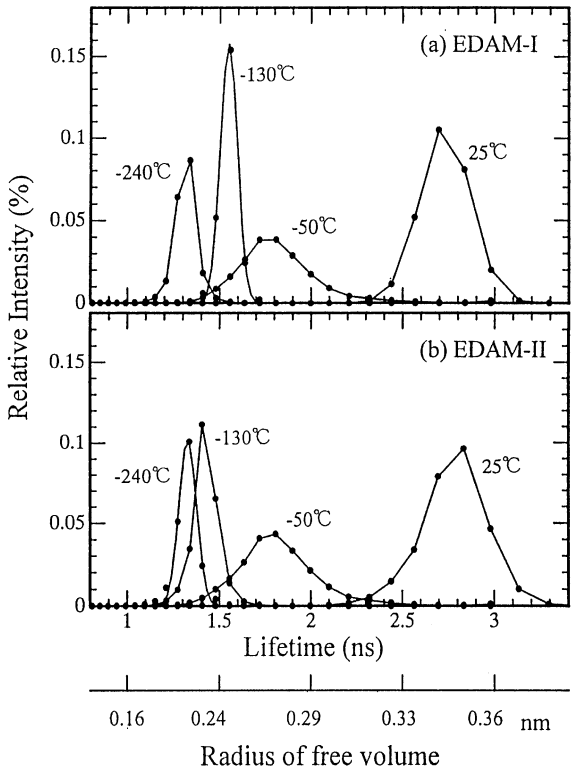

Figure 9. Histograms of the lifetime distribution for EDAM films at the indicated temperatures.

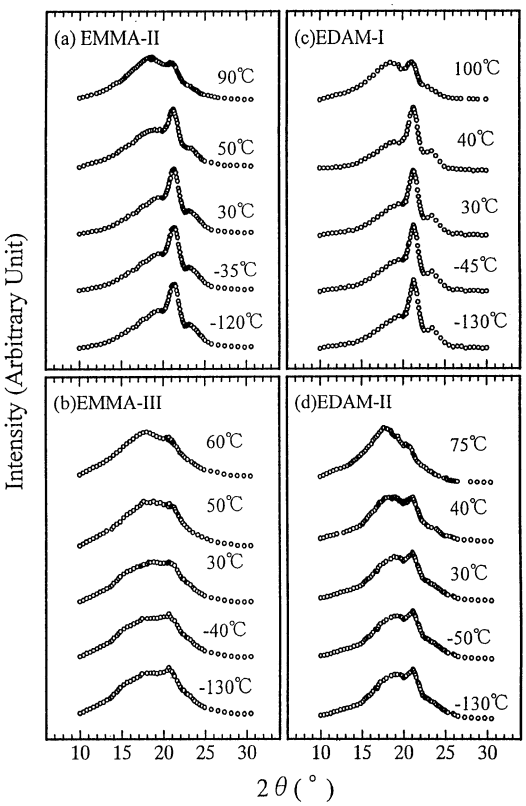

Figure 10. WAXD intensity distributions for EMMA (EMMA-II and EMMA-III) and EDAM (EDAM-I and EDAM-II) films at elevated temperatures.

Table 2. Transition Temperatures of EMMA and EDAM Melt Films

	PALS transition temperature (°C)			β dispersion (°C)	DSC		
specimen	first	second	third	viscoelastic	first	second	third
EMMA-I	−120	−35	48	−26	−30	48	100
EMMA-II	−120	−35	48	−27	−26	45	85
EMMA-III	−125	−40	47	−28	−25	43	64
EDAM-I	−125	−48	38	−41	−42	42	92
EDAM-II	−130	−50	35	−48	−40	36	66

with the second melting peak observed by the DSC curve.

To check the temperature behavior of unstable crystallites of EMMA (EMMA-II and EMMA-III) and EDAM (EDAM-I and EDAM-II), the X-ray intensity distribution was measured from −130 °C to desired temperature beyond 60 °C. The results are shown in Figure 10. The specimens were maintained for 10 min to ensure the accumulation of the intensity. As described in the previous paper,[1] two peaks for EMMA-II appeared at 21.5° and 23.3° (twice the Bragg angle), corresponding to the reflections from the (110) and (200) planes of polyethylene orthorhombic crystals, respectively. The large deviations of peaks corresponding to the (200) plane to lower angle are due to the expansion of the *a*-axis, indicating unstable state of crystallites. The large broad peak at 18.2° is attributed to the contribution from the amorphous phase. The peaks become more intense with increasing temperature. The same tendency was also observed for EDAM. Judging from a small peak in DSC curve (see Figure 1) and the third transition of τ_3 by positron annihilation (see Figures 5 and 6), the temperature relating to the decrease in X-ray diffraction intensity peak corresponds to the temperature associated with the small DSC peak and the third transition of τ_3. Accordingly, there is a small decrease in crystallinity due to the partial melting of small unstable crystallites. Actually, the intensity distribution measured at temperature < −35 °C is similar to that measured at 30 °C. This indicates that the first and second transitions of τ_3, corresponding to the γ and β dispersions, are related to the molecular motions in the amorphous regions. Namely, in addition to the local motion involving the rapid trans−gauche interconversion of the central C−C bond of a short segment (e.g., three to four CH_2), even a large movement of amorphous chains causes no significant effect on crystallinity. This phenomenon was also observed for the branched polyethylene (G201). However, as discussed in the previous paper,[1] the careful observation for EMMA-III reveals that the peak intensity appearing at 21.5° at temperature < −40 °C is slightly higher than that at 30 °C, indicating a slight progression of crystallization. The progression is probably due to the fact that at any temperature there are regions of ethylene-rich sequences that have minimal topological constraints and yet do not crystallize because of the presence of the comonomer. Owing to the rather short ethylene sequences in these regions, stable crystallites cannot form until the temperature drops further. So these regions are likely to be in some dynamic state of order and disorder. Thus, on average, such regions are more ordered than the noncrystalline segments that are additionally constrained by topology.

The profile of the X-ray diffraction intensity at −130 °C is equal to that at −40 °C; −130 °C corresponds to the third transition of τ_3 (see Figure 6b) associated with the local motion of noncrystalline chain segments. Therefore, for all the specimens, no change of X-ray intensity is observed at −40 and −130 °C.

Apart from the above static information, the phase structure of EMMA films was investigated in relation

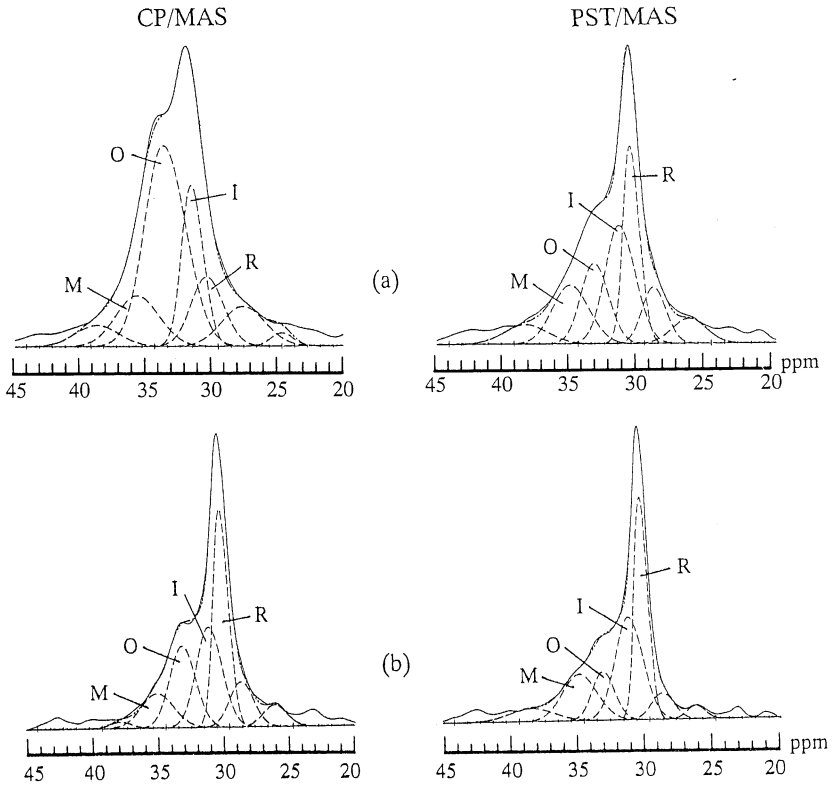

Figure 11. The 67.8 MHz ^{13}C CP/MAS and PST/MAS spectra measured for EMMA-I films (a) at room temperature and (b) 55 °C.

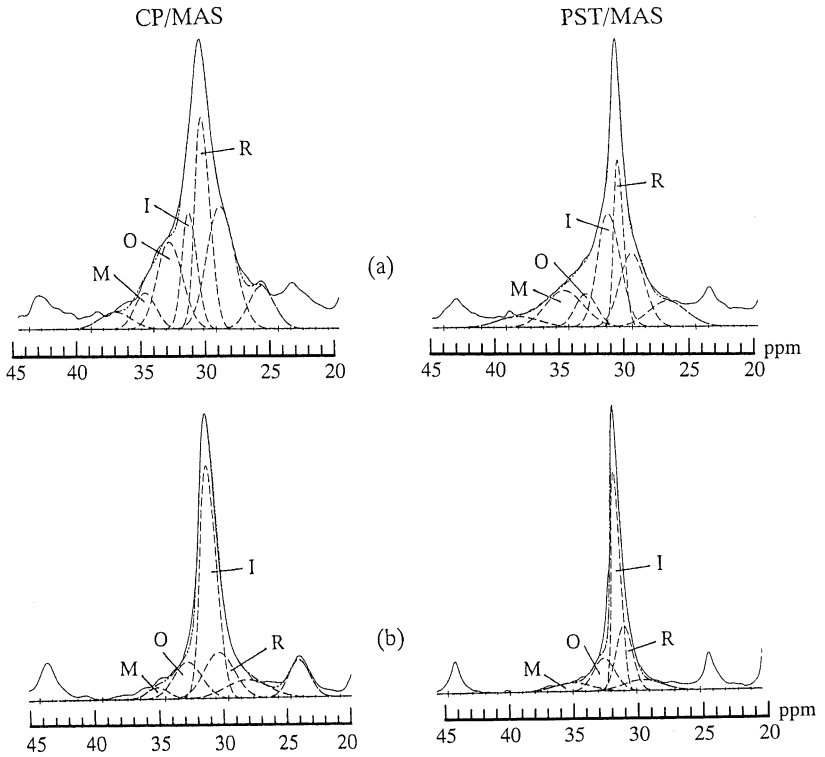

Figure 12. The 67.8 MHz ^{13}C CP/MAS and PST/MAS spectra measured for EMMA-III films at room temperature and (b) 55 °C.

to the molecular mobility of side groups by high-resolution solid-state ^{13}C NMR. Figures 11 and 12 show the 67.8 MHz CP/MAS and PST/MAS ^{13}C NMR spectra of EMMA-I and EMMA-III films, respectively. The measurements were done in the range from 20 to 45 ppm at room temperature and 55 °C. These spectra are shown first to explain the outline of our NMR experiments and to make peak assignment. As described in the previous paper,[1] the CP/MAS spectra show two peaks, peak I (corresponding to peak O in this paper) and II (peak R), which can be assigned to the orthorhombic crystalline and noncystalline methylene carbons in the ethylene sequence, respectively. The assignment of the other peaks was made according to the DD/MAS

Table 3. ^{13}C NMR Chemical Shifts and Mass Fractions of the Respective Components at the Indicated Temperature Measured for EMMA Films[a]

specimen		temp (°C)	chemical shifts (ppm) C_o	C_m	I	R
EMMA-I	CP/MAS	25	33.0	35.2	31.1	30.1
		55	33.0	35.0	31.0	30.2
	PST/MAS	25	33.0	34.8	31.2	30.2
		55	33.0	34.9	31.0	30.2
EMMA-III	CP/MAS	25	32.9	34.8	31.1	30.1
		55	32.9	35.0	30.9	30.2
	PST/MAS	25	32.9	34.7	31.1	30.1
		55	32.8	35.0	31.3	31.1

[a] C_o, orthorhombic crystal film; C_m, monoclibic crystal form; I, interfacial component; R, rubbery component.

spectra of EDAM reported already[1] as well as the solution NMR spectra.[9] All the spectra were analyzed on the basis of the assumption of a superposition curve of Gaussian and Lorentzian functions. In this process, the line width and the peak height of each component were determined to give the best fit by computer on the basis of small changes from the initial peak position. The initial values of the all components were given by adopting the corresponding chemical shifts of EMMA and G201 obtained elsewhere.[1] The corresponding chemical shifts are listed in Table 3. The spectrum indicates the existence of the orthorhombic crystal peak (O), monoclinic crystal peak (M), interfacial component peak (I), and rubbery components peak (R).[42−44] The composite curve is shown by a dotted line, which closely reproduces the observed spectrum (solid line). For EMMA-I, peak O of CP/MAS associated with orthorhombic crystal unit becomes smaller at elevated temperature, indicating a partial melting of unstable crystallites. This tendency is in good agreement with the results of PST/MAS. Namely, the peak R becomes higher at elevated temperature, since PST/MAS spectra are acquired with a short repetition time in order to emphasize the contribution of the amorphous phase. For EMMA-III, the above tendency becomes more remarkable, indicating that the orthorhombic crystal unit within EMMA-III is less stable than that within EMMA-I. These ^{13}C NMR results support the change in X-ray diffraction profile shown in Figure 10.

IV. Conclusions

The relationship between the morphology and the mechanical properties of EMMA films with different MMA contents (EMMA-I with 3.0 mol %, EMMA-II with 6.5 mol %, and EMMA-III with 14.6 mol %) were investigated as a function of temperature by using positron annihilation, X-ray diffraction, and ^{13}C solid-state NMR. To make clear the effect of side groups on the morphology and molecular mobility of EMMA, the characteristics of EDAM and branched polyethylene were discussed together. The positron annihilation data taken in the dark provided clear information on three kinds of transitions from the measurements of intensity (I_3) and lifetime (τ_3) of o-Ps. With increasing temperature, I_3 increased, but around −160 °C, I_3 began to decrease with increasing temperature. I_3 attained to a minimum at around −35 °C. Around −150 and −35 °C were considered to be the temperatures corresponding to the local mode relaxation of ethylene sequence having two different effects on the trapped electron. The former is the commencement to remove trapped electrons from the shallow potential due to the rapid trans−gauche transition of the central C−C bond of a short segment (e.g., three to four CH_2), while the latter is the contribution to the elimination of the shallow potential due to a large motion of polymer chains. The former and the latter transitions were termed as the first and second transitions. The third transition at 40−50 °C is attributed to the partial melting of unstable small crystallites. X-ray results supported that the third transition was related to the partial melting of unstable crystallites. The second and third transitions were confirmed by DSC measurements. Detailed observation of X-ray intensity distribution revealed that, for EMMA-III with the lowest crystallinity, the intensity curves at temperature < −40 °C are slightly different from that at 30 °C. The peak intensity appearing at 21.5° observed at temperatures < −40 °C is slightly higher than that at 30 °C, indicating an increase in crystallinity at lower temperature. The progression is probably due to the fact that at any temperature there are regions of ethylene-rich sequences, with minimal topological constrains, that are close to crystallizing. However, because of the presence of the comonomer and the corresponding finite ethylene sequence length, these regions are in a dynamic state of order/disorder and cannot form stable crystallites until the temperature drops further.

Acknowledgment. We are indebted to Dr. D. L. VanderHart, National Institute of Standards and Technology, for valuable comments and suggestions on the publication of this paper.

References and Notes

(1) Ma, L.; Bin, Y.; Sakai, Y.; Chen, Q.; Kurose, H.; Matsuo, M. *Macromolecules* **2001**, *34*, 4802.
(2) Liu, J.; Deng, Q.; Jean, Y. C. *Macromolecules* **1993**, *26*, 7149.
(3) Simha, R.; Somcynsky, T. *Macromolecules* **1969**, *2*, 342.
(4) Turnbell, D.; Cohen, M. H. *J. Chem. Phys.* **1961**, *34*, 120.
(5) Turnbell, D.; Cohen, M. H. *J. Chem. Phys.* **1970**, *52*, 3038.
(6) Suvegh, K.; Klapper, M.; Domjan, A.; Mullins, S.; Wunderlich, W.; Vertes, A. *Macromolecules* **1999**, *32*, 1147.
(7) Keyser, R. M.; Tsuji, K.; Williams, F. In *The Radiation Chemistry of Macromolecule*; Dole, M., Ed.; Academic Press: New York, 1972; Vol. 1, Chapter 9, pp 149−193.
(8) Ohmae, T.; Hosoda, S.; Tanaka, H.; Kihara, H.; Jiang, B.; Ying, Q.; Qian, R.; Masuda, T.; Nakajima, A. *Pure Appl. Chem.* **1993**, *65*, 1825.
(9) Chen, Q.; Luo, H. J.; Yang, G.; Xu, D. F. *Polymer* **1997**, *38*, 1203.
(10) Luo, H.-J.; Chen, Q.; Yang, G.; Xu, D. *Polymer* **1998**, *39*, 943.
(11) Merrett, F. M. *J. Polym. Sci.* **1957**, *24*, 467.
(12) Matsuo, M.; Sawatari, C.; Ohhata, T. *Macromolecules* **1988**, *21*, 1317.
(13) Sawatari, C.; Matsuo, M. *Polymer* **1989**, *30*, 1603.
(14) Kawai, H.; Suehiro, S.; Kyu, T.; Shimomura, A. *Polym. Eng. Rev.* **1983**, *3*, 10.
(15) Suehiro, S.; Yamada, T.; Inagaki, H.; Kyu, T.; Nomura, S.; Kawai, H. *J. Polym. Sci., Polym. Phys. Ed.* **1979**, *17*, 763.
(16) Matsuo, M.; Ma, L.; Azuma, M.; He, C.; Suzuki, T. *Macromolecules* **2002**, *35*, 3059.
(17) Illers, K. H. *Kolloid Z. Z. Polym.* **1973**, *251*, 394.
(18) Hentschel, D.; Sillescu, H.; Spiess. *Macromolecules* **1981**, *14*, 1607.
(19) Tao, S. J. *J. Phys. Chem.* **1972**, *56*, 5499.
(20) Walender, M.; Maurer, F. H. *J. Mater. Sci. Forum* **1992**, *105*, 1181.
(21) Suzuki, T.; Oki, Y.; Numajiri, M.; Miura, T.; Kondo, K.; Ito, Y. *Radiat. Phys. Chem.* **1995**, *45*, 657.
(22) Levey, B.; Lalovic, M.; Ache, H. J. *J. Chem. Phys.* **1989**, *90*, 3282.
(23) Zhang, Z.; Ito, Y. *Radiat. Phys. Chem.* **1991**, *38*, 221.
(24) Suzuki, T.; Oshima, N.; Miura, T.; Oki, Y.; Numajiri, M. *Polymer* **1997**, *37*, 5521.
(25) Uedono, A.; Kawano, T.; Tanigawa, S.; Ban, M.; Kyoto, M.; Uozumi, T. *J. Polym. Sci., Part B* **1997**, *35*, 1601.

(26) van Krevelen, D. W.; Hoftyzer, P. J. *Properties of Polymers*; Elsevier Publications Co.: Amsterdam, 1976.
(27) Serna, J.; Abbe, J. Ch.; Duplatre, G. *Phys. Status Solidi* **1989**, *A115*, 389.
(28) Suzuki, T.; Hayashi, T.; Ito, Y. *Mater. Res. Innov.* **2001**, *4*, 273.
(29) Hirade, T.; Kumada, T. *Radiat. Phys. Chem.* **2001**, *60*, 541.
(30) Mogensen, O. E. In *Positron Annihilation in Chemistry*; Springer-Verlag: Berlin, 1995.
(31) Ito, Y. J. *Radianal. Nucl. Chem.* **1996**, *210*, 327.
(32) Kobayashi, Y.; Wang, C. L.; Hirata, K.; Zheng, W.; Zhang, C. *Phys. Rev. B* **1998**, *58*, 5384.
(33) Nagai, Y.; Hasegawa, M.; Kobayashi, Y.; Wang, C. L.; Zheng, W.; Zhang, C. *Phys. Rev.* **1999**, *B60*, 11863.
(34) Suzuki, T.; He, C.; Shantarovich, V.; Kondo, K.; Hamada, E.; Matsuo, M.; Ma, L.; Ito, Y. *Radiat. Phys. Chem.*, in press.
(35) Bursa, R. S.; Duarte Naia, M.; Margoni, D.; Zecca, A. *Appl. Phys.* **1995** *A60*, 447.
(36) Hirrade, T.; Maurer, F. H.; Eldrup, M. *Radiat. Phys. Chem.* **2000**, *58*, 465.
(37) Suzuki, T.; He, C.; Kondo, E.; Hamada, Matsuo, M.; Ma, L.; Ito, Y. *Radiat. Phys. Chem.*, in press.
(38) Ito, Y.; Hirade, T.; Hamada, E.; Suzuki, T.; Ito, Y. *Acta Phys. Pol.* **1999**, *A95*, 533.
(39) Chen, Z. O.; Suzuki, T.; Kondo, K.; Uedono, A,; Ito, Y. *Jpn. J. Appl. Phys.* **2001**, *40*, 5036.
(40) Suzuki, T.; Kondo, K.; Hamada, E.; Ito, Y. *Radiat. Phys. Chem.* **2000**, *58*, 465.
(41) Shukla, A.; Hoffmann, L.; Manuel, A. A.; Peter, M. *Mater. Sci. Forum* **1997**, *255*, 233.
(42) Earl, W. L.; VanderHart, D. L. *Macromolecules* **1979**, *12*, 762.
(43) VanderHart, D. L.; Khoury, F. *Polymer* **1984**, *25*, 1589.
(44) Ando, I.; Yamanobe, T.; Sorita, T.; Komoto, T.; Sato, H.; Deguchi, K.; Imanari, M. *Macromolecules* **1984**, *17*, 1955.

MA021543R